

Searching for lepton flavor violating interactions at future electron-positron colliders

S. M. Etesami, R. Jafari, M. Mohammadi Najafabadi, S. Tizchang

School of Particles and Accelerators, Institute for Research in Fundamental Sciences (IPM) P.O. Box 19395-5531, Tehran, Iran

Abstract

Lepton flavor violating interactions are absent in the standard model but are expected in various beyond standard models. In this work, the potential of the future circular electron-positron collider to probe the four fermion lepton flavor couplings via the $e^+e^- \rightarrow e^\pm\tau^\mp$ process is revisited by means of an effective field theory approach. We provide constraints at 95%CL on the dimension-six Wilson coefficients including major sources of background processes and considering realistic detector effects at four expected operation energies $\sqrt{s} = 157.5, 162.5, 240$ and 365 GeV according to their corresponding integrated luminosities. We demonstrate that statistical combination of the results from four center-of-mass energies, improve the sensitivity to the LFV couplings significantly. We compare the results with the prospects from Belle II with 50 ab^{-1} and other studies at electron-positron colliders.

Keywords: Lepton flavor violation, lepton collider

1 Introduction

In the standard model (SM) with massless neutrinos, processes with lepton flavor violating (LFV) interactions are forbidden [1]. However, experimental observations of neutrino oscillations show that neutrinos are massive and mix with each other which leads to violation of lepton flavor conservation [2]. LFV enters into the charged lepton sector from the neutrino sector via radiative corrections which are extremely suppressed because of the smallness of the ratio of neutrino mass to the W boson mass [3, 4]. The predicted branching fraction for example for $\tau^- \rightarrow \ell^+ \ell^- \ell'^-$ decays are approximately $\lesssim 10^{-54}$, where $\ell = e, \mu$ [4]. However, an increase of several orders of magnitude is predicted in some extensions of the SM, such as supersymmetric SM [5–7], resulting in branching fractions observable at experiments. Therefore, any observation of LFV in the charged lepton sector would be an obvious hint to the presence of physics beyond the SM, and can be an indirect way to search for beyond the SM scenarios.

So far, no LFV interactions among the charged leptons have been observed and there are several strong constraints from various experiments. For instance, $\ell^- \rightarrow e^- e^+ e^-$, $\ell \rightarrow e \gamma$ with $\ell = \tau, \mu$, rare decays of mesons, Z boson decays, decays of Higgs boson and heavy resonances have been used to probe LFV in different experiments [8–17]. The most stringent bounds at 90% CL on the LFV decays of the τ leptons into $3e$ were measured by BaBar and Belle [18, 19]:

$$\mathcal{B}(\tau^- \rightarrow e^- e^+ e^-) \leq 2.9 \times 10^{-8} \text{ (BaBar)}, \quad \mathcal{B}(\tau^- \rightarrow e^- e^+ e^-) \leq 2.7 \times 10^{-8} \text{ (Belle)}, \quad (1)$$

The Belle II future prospects for upper limit on $\mathcal{B}(\tau^- \rightarrow e^- e^+ e^-)$ at 90% CL assuming the integrated luminosity of 50 ab^{-1} is $\lesssim 10^{-10}$ [20].

The proposed future lepton colliders such as the International Linear Collider (ILC) [21–23], the Compact Linear Collider (CLIC) [24–26], Circular Electron-Positron Collider (CEPC) [27, 28] and Future Circular Collider with electron-positron collisions (FCC-ee) with highest-luminosity [29] are expected to provide an extraordinary place to perform flavor physics studies. There are a variety of theories that give rise to LFV. For instance, additional fermions present in the type III seesaw model or in the low-scale seesaw models give rise to large LFV effects [30–32]. The LFV through Z, Higgs boson, and other new degrees of freedom have been studied in Refs. [33–36], and Higgs and scalar LFV decays have been presented in Refs. [37–40]. If the new degrees of freedom contributing to LFV are heavy comparing to the energy accessible at colliders then the LFV couplings could be reasonably parameterized via the effective contact interactions. Experiments can perfectly search for LFV in a model-independent approach, without any theoretical input. Effective field theories allow for a model-independent interpretation of the experimental results. However, in a true bottom-up approach, all relevant operators have to be considered since no symmetry or model consideration is present to suppress some operators with respect to other operators.

LFV $e\bar{e}\tau$ contact interactions have been already studied at future high energy lepton colliders through $e^+e^- \rightarrow e^\pm\tau^\mp$ in Refs. [41, 42]. In Ref. [42], the LFV contact operators probed via $e^+e^- \rightarrow e^\pm\tau^\mp$ process at $\sqrt{s} = 250, 500, 1000, 3000 \text{ GeV}$ considering two main background sources, $\tau^+\tau^-$ and $e\tau\nu_e\nu_\tau$. Similar process examined at $\sqrt{s} = 250, 500, 1000 \text{ GeV}$ in Ref. [42] where the effects of polarization of the electron and positron beam have been investigated. The detector response has been simulated using **Delphes** package [43] and $e^\pm\tau^\mp\nu_e\nu_\tau$ has been considered as the main source of background.

The purpose of this paper is to investigate the LFV contact interactions of $e\bar{e}e\bar{\tau}$ at a future lepton collider. In particular, the focus is on a model independent search for various types of four-lepton LFV interactions leading to the production of $e^\pm\tau^\mp$ at the future circular electron-positron

collider. The search is performed at the proposed energies and integrated luminosity benchmarks of the FCC-ee. Particularly, the analysis is carried out at the center of mass energies of 157.5, 162.5, 240 and 365 GeV with the corresponding integrated luminosities of 5, 5, 5, and 1.5 ab^{-1} , respectively. A realistic detector response is taken into account using **Delphes** package. The main sources of background processes are $\tau^+\tau^-$, $e^\pm\tau^\mp\nu_e\nu_\tau$, $\ell^\pm\ell^\mp\ell'^\pm\ell'^\mp$, $\ell^\pm\ell^\mp jj$, $\ell\nu jj$, ($\ell = e, \mu, \tau$), and jj , ($j = \text{jet}$). Finally, a statistical combination is performed over the results obtained at the four center-of-mass energies.

The layout of this paper is as follows. In section 2 the effective operators describing LFV are briefly presented. Section 3 is dedicated to present the simulation details and analysis strategy. In section 4, the constraints on LFV couplings and the results of statistical combinations are given. Finally, section 5 concludes the paper.

2 The LFV effective Lagrangian

For studying the $\bar{e}e\bar{e}\tau$ LFV couplings, it is customary in the literature to consider four fermi contact interactions which provide the opportunity to characterize the new physics effects in a model-independent framework. In general, there is a set of six chirality conserving scalar and vector form four-fermi operators with $\Delta L = 1$ where ΔL represents the difference between initial and final state lepton numbers [44]. The operators are classified into two types: the scalar type (S) and vector type (V) interactions. In addition, there are LFV operators containing dipole structures which are tightly constrained by radiative LFV decays [45], therefore, they are not considered in this work. The effective Lagrangian and the relevant set of operators leading to $e^\pm\tau^\mp$ production by either a scalar or vector are given by [44]:

$$\mathcal{L}_{\text{eff}} \supset \sum_{\alpha,\beta} \sum_{ij} \frac{c_{\alpha\beta}^{ij}}{\Lambda^2} \mathcal{O}_{\alpha\beta}^{ij}, \quad (2)$$

$$\begin{aligned} \mathcal{O}_{RL}^{S,ij} &= (\bar{\ell}_{jL}\ell_{iR}) (\bar{\ell}_{jL}\ell_{jR}), & \mathcal{O}_{LR}^{S,ij} &= (\bar{\ell}_{iR}\ell_{jL}) (\bar{\ell}_{jR}\ell_{jL}), \\ \mathcal{O}_{RR}^{V,ij} &= (\bar{\ell}_{iR}\gamma^\mu\ell_{jR}) (\bar{\ell}_{jR}\gamma_\mu\ell_{jR}), & \mathcal{O}_{LL}^{V,ij} &= (\bar{\ell}_{iL}\gamma^\mu\ell_{jL}) (\bar{\ell}_{jL}\gamma_\mu\ell_{jL}), \\ \mathcal{O}_{LR}^{V,ij} &= (\bar{\ell}_{iL}\gamma^\mu\ell_{jL}) (\bar{\ell}_{jR}\gamma_\mu\ell_{jR}), & \mathcal{O}_{RL}^{V,ij} &= (\bar{\ell}_{iR}\gamma^\mu\ell_{jR}) (\bar{\ell}_{jL}\gamma_\mu\ell_{jL}), \end{aligned} \quad (3)$$

where $\mathcal{O}_{\alpha\beta}^{ij}$ are the four fermion leptonic operators, Λ is the new physics energy scale, and $c_{\alpha\beta}^{ij}$ s indicate the effective Wilson coupling between leptons of flavor i and j and $\alpha\beta$ Lorentz structures. The operators are invariant under the SM gauge symmetry $\text{SU}(3) \times \text{SU}(2) \times \text{U}(1)$. It is found that flavor violation among first and second generations of leptons is tightly constrained by experimental constraints arising from muon decay into three electron $\mu \rightarrow eee$ at SINDRUM experiment [46], the muon transition to $e\gamma$ [47], and $\mu - e$ conversion [48]. However, constraints on flavor violations between electron and τ and, muon and τ are much looser. As a consequence, we restrict our study to $\bar{e}e\bar{e}\tau$ couplings using $e^-e^+ \rightarrow e^\pm\tau^\mp$ process.

In addition to the $\bar{e}e\bar{e}\tau$ four fermi contact interactions, contact interactions among leptons and quarks (like $\bar{e}e\bar{q}q'$), and electrons and Higgs- Z ($eeHZ$) are of favourite topics which have been probed in several papers such as Refs. [49–52].

In order to see the dependence of the production rate to the center of mass energy \sqrt{s} and to find a feeling about the sensitivity to different types of operators, the expression for the cross section of $e^-e^+ \rightarrow e^\pm\tau^\mp$ process is presented. The theoretical cross section of $\sigma(e^-e^+ \rightarrow e^\pm\tau^\mp) +$

$\sigma(e^-e^+ \rightarrow e^-\tau^+)$ in the presence of all couplings has the following form [53]:

$$\sigma(s) = \frac{s}{96\pi\Lambda^4} \left\{ (|c_{LR}^S|^2 + |c_{RL}^S|^2) + 16(|c_{LL}^V|^2 + |c_{RR}^V|^2 + |c_{LR}^V|^2 + |c_{RL}^V|^2) \right\}. \quad (4)$$

where in finding the above expression, the lepton masses are set to zero considering the center-of-mass energy scale. As seen, production rate of the four-fermion interactions grows linearly with the squared center-of-mass energy s , and diverge when $s \rightarrow \infty$. However, one should note that we are working in a non-renormalizable formalism and these operators provide an acceptable description of physics at high energy up to an energy scale Λ . Another interesting point which is worth mentioning is that the vector type operators contribute to LFV production of $e\tau$ with a factor of 16 larger than the scalar type operators. Therefore, better sensitivity is expected to vector type with respect to scalar type operators.

In the next section, we describe the simulation method and details of the analysis to search for the LFV operators at four energy benchmarks of the FCC-ee.

3 Simulation details and analysis strategy

The main goal of this work is to estimate the potential of the proposed FCC-ee collider to probe the effective LFV operators introduced in Eq.2 using $e^-e^+ \rightarrow e^\pm\tau^\mp$ process. This section is dedicated to present event generation, simulation of detector effects and analysis method to find the LFV sensitivity for four energy benchmarks. In particular, the search is separately performed at center-of-mass energies 365, 240, 162.5 and 157.5 GeV with their expected integrated luminosities of 1.5, 5, 5 and 5 ab^{-1} at FCC-ee collider, respectively [29]. The signal process consists of an electron (or a positron) and a $\bar{\tau}$ lepton (or a τ lepton) which decays hadronically. The main background sources which are taken into account in this study are:

- (I) $e^-e^+ \rightarrow e^\pm\tau^\mp\nu\bar{\nu}$,
- (II) $e^-e^+ \rightarrow \tau^+\tau^-$,
- (III) $e^-e^+ \rightarrow \ell^\pm\ell^\mp\ell'^\pm\ell'^\mp$ ($\ell, \ell' = e, \mu, \tau$),
- (IV) $e^-e^+ \rightarrow \ell^\pm\ell^\mp jj$ ($\ell = e, \mu, \tau$),
- (V) $e^-e^+ \rightarrow \ell^\pm\nu jj$ ($\ell = e, \mu, \tau$),
- (VI) $e^-e^+ \rightarrow jj$.

The second background, $\tau^+\tau^-$, is in particular contributing to the background composition when one of the τ leptons decay to an electron and the electron is reconstructed in the final state. The third item in the list of backgrounds, $\ell^\pm\ell^\mp\ell'^\pm\ell'^\mp$, is considered as there is a possibility that two of the leptons are scattered to regions of pseudorapidity where detector area is blind or two isolated charged leptons are not well reconstructed. Since jets can be misidentified as electrons and also as τ leptons, the fourth to sixth items must be included in the list of backgrounds to obtain a more realistic assessment of the results.

The effective Lagrangian introduced in Eq. 2 is implemented in the **FeynRule** program [55] and then the Universal FeynRules Output (UFO) model [56] is inserted to **MadGraph5_aMC@NLO 2.6.6**. The events of signal and backgrounds are generated at leading order with **MadGraph5_aMC@NLO 2.6.6** [57–59] including ISR effect. The ISR effects are considered using the **MGISR** plugin in **MadGraph5_aMC@NLO 2.6.6** [60, 61]. The generated events are passed through **PYTHIA 8** [62, 63] for showering, hadronization, and decay of unstable particles. The detector effects are simulated via **Delphes 3.4.2** [43] according to an ILD-like detector [64]. For electrons with $p_T > 10$ GeV

\sqrt{s} [GeV]	$c_{LR}^V = 0.1$	$c_{LR}^S = 0.1$	$e\tau\nu\bar{\nu}$	$\tau\bar{\tau}$	$\ell\bar{\ell}\ell'\bar{\ell}'$	$\ell\bar{\ell}jj$	$\ell\nu jj$	jj
157.5	4.72 ± 0.007	0.29 ± 0.0004	22.33 ± 0.07	11076.5 ± 3.4	39.86 ± 0.08	80.95 ± 0.2	272.9 ± 0.4	32032 ± 8.1
162.5	5.02 ± 0.007	0.31 ± 0.0004	102.12 ± 0.3	10275.8 ± 2.9	42.23 ± 0.08	83.06 ± 0.3	1198.05 ± 0.8	29133 ± 6.2
240	10.98 ± 0.04	0.69 ± 0.0008	415.63 ± 0.6	4196.8 ± 1.2	86.24 ± 0.2	217.8 ± 0.5	4552.7 ± 1.3	10481 ± 3.5
365	25.26 ± 0.07	1.57 ± 0.002	327.59 ± 0.5	1803.6 ± 0.6	85.05 ± 0.1	195.13 ± 0.3	3247.02 ± 1.1	4306 ± 1.2

Table 1: The cross sections of signal $e^-e^+ \rightarrow e^\pm\tau^\mp$ and main background processes with their corresponding uncertainties are presented. The cross section of two signal scenarios are given assuming $c_{LR}^V = 0.1$, $c_{LR}^S = 0.1$, and $\Lambda = 1$ TeV. The cross sections are in unit of fb and are after including the ISR effects.

and $|\eta| \leq 2.5$, the identification efficiency in the ILD card is 95%. The electron energy resolution is: $\frac{\Delta E}{E} = \frac{0.15}{\sqrt{E}} + 0.01$. To calculate the cross section of signal and backgrounds and simulate the events, the SM relevant input values are set as follows: $M_Z = 91.188$ GeV, mass of τ lepton $m_\tau = 1.777$ GeV, $G_F = 1.166 \times 10^{-5}$ GeV $^{-2}$, $\alpha_e = 1/127.9$, and $\alpha_s = 0.118$.

The τ lepton lifetime is ~ 290 femto second, corresponding to $c\tau \sim 87\mu m$. The actual decay length is obtained by multiplying $c\tau$ with $\beta\gamma$ therefore a τ lepton with $E = 40$ GeV travels around 2 mm through the detector then decays. In around two thirds of decays, τ 's decay hadronically, typically to one or three charged mesons (mostly $\pi^-\pi^+$), often associated with neutral pions, and a τ neutrino. The τ tagging efficiency in the ILD simulation card is 40% and the τ misidentification rate is assumed to be equal 0.1% [65].

Six different signal samples corresponding to the six operators presented in Eq.3 are generated. In order to generate signal events, we set related effective Wilson coefficient $c_{ij} = 0.1$, with $i = j = L, R$, and $\Lambda = 1$ TeV and require pre-selection cuts as $p_T^\ell = 10$ GeV, pseudorapidity of leptons $|\eta^\ell| < 3.0$ and angular separation between two leptons as $\Delta R = \sqrt{(\Delta\eta)^2 + (\Delta\phi)^2} > 0.3$. For generating the background samples, we require the addition of angular separation between leptons and jets, and two jets in the final state to be $\Delta R_{\ell,j} > 0.3$ and the $p_T = 10$ GeV and $|\eta| < 3.0$ are applied on jets in the final state at generator level.

The cross-section and corresponding uncertainties with ISR effect of backgrounds as well as signals are given in Table 1 for all center-of-mass energies 157.5, 162.5, 240 and 365 GeV.

The signal events are selected according to the following requirements. We ask for exactly two leptons with opposite charge, one isolated electron and one τ -tagged lepton. It is required that $p_T^e > 10$ GeV, $p_T^\tau > 20$ GeV and pseudorapidity of both leptons must satisfy $|\eta^\ell| < 2.5$. and $\Delta R_{e,\tau} > 0.5$. In order to make sure the electron candidate is well isolated, it is required $\text{RelIso} < 0.15$, where RelIso is defined as the ratio of the sum of p_T of charged particle tracks inside a cone of size 0.5 around the electron track to p_T of the electron. τ leptons which decay via hadronic modes are considered. A τ lepton in hadronic decay mode produces a jet containing a few neutral and charged hadrons. Therefore, considering the τ tagging efficiency, a jet is considered potentially as a τ candidate if a generated τ exists within a distance $\Delta R = \sqrt{(\eta_{\text{jet}} - \eta_\tau)^2 + (\phi_{\text{jet}} - \phi_\tau)^2} = 0.3$ from the jet axis.

To suppress the contributions from events with e^-e^+ and $\mu^-\mu^+$ in the final state, events that contain two electron or two muon candidates are rejected. This reduces background events from $\ell^\pm\ell^\mp\ell'^\pm\ell'^\mp$, $\ell^\pm\ell^\mp jj$, and $\tau^+\tau^-$ with $\tau \rightarrow e\nu_e\nu_\tau$ or $\tau \rightarrow \mu\nu_\mu\nu_\tau$.

To enhance the sensitivity, we apply additional cuts on the energy of final state electron and the invariant mass of the two leptons $M_{e\tau}$. Figure 1 displays the distributions of the electron energy in the final state (left plot) and invariant mass of final state, i.e. $M_{e\tau}$ (right plot) at a center-of-mass energy of 240 GeV. Obviously, both distributions show significant difference between the shape of signal and background processes. The $M_{e\tau}$ distributions for $\ell^\pm\ell^\mp jj$, $\tau^+\tau^-$

and $\ell^\pm \ell^\mp \ell'^\pm \ell'^\mp$ background processes peak at lower values with respect to the signal and even the other backgrounds. This is expected as the center-of-mass energy is shared among at least four particles in $\ell^\pm \ell^\mp jj$ and $\ell^\pm \ell^\mp \ell'^\pm \ell'^\mp$ processes. Therefore, cutting on $M_{e\tau}$ suppresses effectively these reducible backgrounds. It is notable that the $M_{e\tau}$ distribution has different behaviours for c_{LL}^V and c_{LR}^V which arises from the fact that for LL coupling $d\sigma/d\cos\theta \propto (1 + \cos\theta)^2$ while for LR coupling $d\sigma/d\cos\theta \propto (1 - \cos\theta)^2$. For the signal events, the energy distribution of the electron is expected to spread around $\sqrt{s}/2$. As a result, it is used to further reduce the contributions of the background processes.

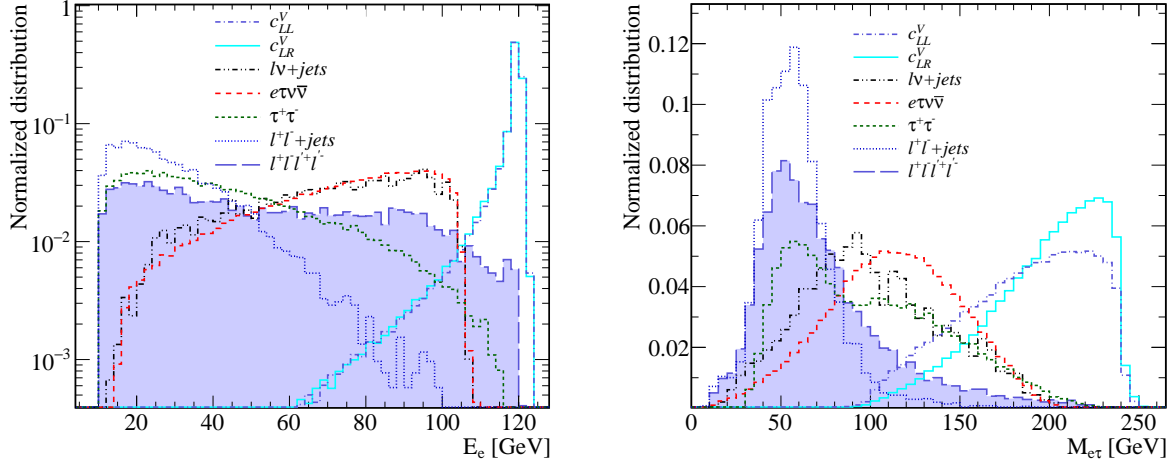


Figure 1: Normalized distributions of electron energy(left), and invariant mass of two final state charged leptons $M_{e\tau}$ (right) are presented for signal benchmarks $c_{LL}^V = 0.1$ and $c_{LR}^V = 0.1$, at $\sqrt{s} = 240$ GeV.

The cut values on E_e and $M_{e\tau}$ are optimized such that the best limit on the LFV coefficients are obtained. In order to optimize the cuts on the invariant mass and energy of the outgoing electron, the upper bound on the signal cross section for different cut values on $M_{e\tau}$ and E_e is obtained. The values which gives lowest upper bound on signal cross section are chosen as the optimum values. The cuts on invariant mass of final state $M_{e\tau}$ are found to be greater than 65 GeV, 100 and 150 GeV for $\sqrt{s} = 157.5 - 162.5$, 240 and 365 GeV, respectively. The optimized lower cuts on energy of electron are obtained to be 78.6, 81.0, 119.7 and 182.0 GeV for $\sqrt{s} = 157.5$, 162.5, 240 and 365 GeV, respectively. Table 2 presents the efficiencies of signal with $c_{LR}^V = 0.1$, $c_{LL}^S = 0.1$ and the main SM backgrounds after preselection cuts, $M_{e\tau}$, and E_e with $\sqrt{s} = 157.5$, 162.5, 240 and 365 GeV. After applying the cuts, the main background contributions arise from $\ell^\pm \ell^\mp \ell'^\pm \ell'^\mp$, $\tau^+\tau^-$ and $\ell^\pm \ell^\mp jj$ and the rest are remarkably suppressed.

As previously indicated, jets could be misidentified as τ and electron therefore, processes with jets in the final state contribute to the background. The detectors proposed for the future lepton colliders are expected to have a great performance better than the current modern multipurpose detectors such as ATLAS and CMS detectors. The jet fake τ probability is expected to be 0.1% [65]. The rate of background containing jets varies with the center-of-mass energy and is assessed to be less than 5% of the total background contributions after all selection criteria.

In the next section, we evaluate the potential sensitivities to LFV operators at four energy benchmarks. In addition, a statistical combination of four center-of-mass energies is presented.

$\sqrt{s} = 157.5 \text{ GeV}$	Signal		SM Backgrounds				
	$c_{LR}^V = 0.1$	$c_{LR}^S = 0.1$	$e\tau\nu\bar{\nu}$	$\tau\bar{\tau}$	$\ell\ell\ell'\ell'$	$\ell\ell jj$	$\ell\nu jj$
(I): Pre-selection cuts	0.1746	0.1698	0.099	0.045	4.9×10^{-3}	1.4×10^{-3}	3.3×10^{-4}
(II): $M_{e\tau} > 65 \text{ GeV}$	0.1741	0.1697	0.038	0.019	2.2×10^{-3}	1.8×10^{-4}	7.5×10^{-5}
(III): $E_e > 78.6 \text{ GeV}$	0.0984	0.0831	2.8×10^{-8}	1.5×10^{-7}	6.02×10^{-6}	1.7×10^{-7}	0.0
$\sqrt{s} = 162.5 \text{ GeV}$	Signal		SM Backgrounds				
	$c_{LR}^V = 0.1$	$c_{LR}^S = 0.1$	$e\tau\nu\bar{\nu}$	$\tau\bar{\tau}$	$\ell\ell\ell'\ell'$	$\ell\ell jj$	$\ell\nu jj$
(I): Pre-selection cuts	0.1727	0.1711	0.106	0.048	4.9×10^{-3}	1.6×10^{-3}	4.5×10^{-4}
(II): $M_{e\tau} > 65 \text{ GeV}$	0.1727	0.1710	0.041	0.025	2.4×10^{-3}	2.1×10^{-4}	1.0×10^{-4}
(III): $E_e > 81 \text{ GeV}$	0.1122	0.0949	6×10^{-8}	2.0×10^{-7}	3.61×10^{-6}	2.1×10^{-7}	0.0
$\sqrt{s} = 240 \text{ GeV}$	Signal		SM Backgrounds				
	$c_{LR}^V = 0.1$	$c_{LR}^S = 0.1$	$e\tau\nu\bar{\nu}$	$\tau\bar{\tau}$	$\ell\ell\ell'\ell'$	$\ell\ell jj$	$\ell\nu jj$
(I): Pre-selection cuts	0.2156	0.2137	0.131	0.037	8.8×10^{-3}	6.2×10^{-3}	4.9×10^{-4}
(II): $M_{e\tau} > 100 \text{ GeV}$	0.2150	0.2134	0.084	0.017	1.6×10^{-3}	2.4×10^{-4}	2.0×10^{-4}
(III): $E_e > 119.7 \text{ GeV}$	0.1072	0.0989	2.1×10^{-8}	1.5×10^{-7}	1.2×10^{-5}	2.4×10^{-7}	0.0
$\sqrt{s} = 365 \text{ GeV}$	Signal		SM Backgrounds				
	$c_{LR}^V = 0.1$	$c_{LR}^S = 0.1$	$e\tau\nu\bar{\nu}$	$\tau\bar{\tau}$	$\ell\ell\ell'\ell'$	$\ell\ell jj$	$\ell\nu jj$
(I): Pre-selection cuts	0.2093	0.2097	0.133	0.066	0.012	6.0×10^{-3}	5.0×10^{-4}
(II): $M_{e\tau} > 150 \text{ GeV}$	0.2053	0.2051	0.093	0.041	2.0×10^{-3}	1.5×10^{-4}	2.4×10^{-4}
(III): $E_e > 182 \text{ GeV}$	0.0993	0.0986	2.6×10^{-8}	3.2×10^{-7}	2.6×10^{-5}	1.4×10^{-7}	0.0

Table 2: The efficiencies for signal with $c_{LR}^V = 0.1$, $c_{LR}^S = 0.1$ and the SM backgrounds after selection cuts with $\sqrt{s} = 157.5, 162.5, 240$ and 365 GeV are given.

4 Results

The CL_s technique [66,67] is exploited to find upper limits on the signal cross section at 95% CL. Then the limits on the signal rates are translated into the upper limits on the LFV couplings. In the CL_s method, we define log-likelihood functions L_{Bkg} and $L_{\text{Signal+Bkg}}$ for the background hypothesis, and for the signal+background hypothesis as the multiplication of Poissonian likelihood functions. The p -value for hypothesis of signal+background and for the background hypothesis are determined using the log-likelihood ratio $Q = -2\ln(L_{\text{Signal+Bkg}}/L_{\text{Bkg}})$. The signal cross section is constrained using $\text{CL}_s = P_{\text{Signal+Bkg}}(Q > Q_0)/(1 - P_{\text{Bkg}}(Q < Q_0)) \leq 0.05$ which is corresponding to 95% confidence level where Q_0 is the expected value of test statistics Q . The RooStats package [68] is used to perform the numerical evaluation of the CL_s.

The predicted constraints at 95% CL for $\sqrt{s} = 157.5 \text{ GeV}$ with $\mathcal{L} = 5 \text{ ab}^{-1}$, $\sqrt{s} = 162.5 \text{ GeV}$ with $\mathcal{L} = 5 \text{ ab}^{-1}$, $\sqrt{s} = 240 \text{ GeV}$ with $\mathcal{L} = 5 \text{ ab}^{-1}$ and $\sqrt{s} = 365 \text{ GeV}$ with $\mathcal{L} = 1.5 \text{ ab}^{-1}$ are presented in Table 3. These results are obtained considering only statistical uncertainties and the impacts of systematic and theoretical sources are neglected. For illustration, the results are also given in Figure 2. As seen, the most sensitivity is achieved on vector type LFV couplings, i.e. on c_{LL}^V , c_{RR}^V , c_{RL}^V , and c_{LR}^V . This is expected as the production rates for the vector type LFV couplings are larger than the scalar type by a factor of 16. Among various center-of-mass energy scenarios, better sensitivity is expected to be obtained from $\sqrt{s} = 365 \text{ GeV}$ for which the signal cross section is largest as $\sigma(e^-e^+ \rightarrow e\tau) \propto s$. Although, less amount of data is planned to be collected at $\sqrt{s} = 365 \text{ GeV}$ with respect to the other energies, similar sensitivity to other energies at $\sqrt{s} = 365 \text{ GeV}$ is obtained.

To achieve better sensitivity, the results from four energy benchmarks are combined using the method explained in Ref. [69]. The combined limits are given in Table 3 and Figure 2. One can see

that the statistical combination of four energy scenarios improves the bounds by almost a factor of around 3 to 4 with respect to the results from a single energy benchmark. It is informative to compare the results from prospects of Belle II with an integrated luminosity of 50 ab^{-1} . The limits from combination are competitive with those expected from Belle II. Finally, we compare the results with those which are expected from a future lepton collider at $\sqrt{s} = 1 \text{ TeV}$ with polarized beams such that $P(e^-) = 0.8$ and $P(e^+) = -0.3$ [42]. The results of combination are sensibly better for both the scalar and vector types of the LFV couplings.

$\sqrt{s} \text{ (GeV)}, \mathcal{L} \text{ (ab}^{-1}\text{)}$	$\frac{c_{LL}^V}{\Lambda^2} [\times 10^{-9}]$	$\frac{c_{RR}^V}{\Lambda^2} [\times 10^{-9}]$	$\frac{c_{LR}^V}{\Lambda^2} [\times 10^{-9}]$	$\frac{c_{RL}^V}{\Lambda^2} [\times 10^{-9}]$	$\frac{c_{LL}^S}{\Lambda^2} [\times 10^{-9}]$	$\frac{c_{RR}^S}{\Lambda^2} [\times 10^{-9}]$
157.5, 5	5.82	5.46	5.74	5.36	21.18	22.61
162.5, 5	5.71	5.36	5.62	5.29	21.42	23.12
240, 5	3.69	3.50	3.73	3.53	14.81	14.74
365, 1.5	3.93	3.94	3.92	3.93	15.80	15.80
Combination	1.32	1.25	1.32	1.25	5.1	5.3
Belle II	1.06	1.06	1.55	1.55	4.29	4.29
$\sqrt{s} = 1 \text{ TeV, pol. beam}$	4.3	1.1	1.6	1.8	13	5.9

Table 3: The 95% CL expected upper bounds on the scalar and vector type LFV couplings assuming four center-of-mass energies as well as the combination are shown. The limits are in the unit of GeV^{-2} . The Belle II future prospects [20] and the expectation from e^-e^+ collider at $\sqrt{s} = 1 \text{ TeV}$ with polarized beam [42] are presented as well.

In order to have a feeling about the impact of systematic uncertainties on the results, we consider conservative values of uncertainties and re-estimate the sensitivities to the LFV couplings. In Ref. [70], a search for LFV events at LEP2 with the OPAL detector using a similar final state as this work has been performed. The analysis has used the full data collected with OPAL at \sqrt{s} between 189 GeV and 209 GeV. The systematic uncertainty on the signal efficiency is 3.5% and on the number of expected background events is 5%. While for the future experiments, the measurements are expected to be made with more accuracy, we consider a conservative value of 5% uncertainty on both signal selection efficiency and on background expectation. The constraints on c_{LL}^V/Λ^2 , c_{RR}^V/Λ^2 , c_{RL}^V/Λ^2 , c_{LR}^V/Λ^2 , c_{RL}^S/Λ^2 , c_{LR}^S/Λ^2 , derived at $\sqrt{s} = 365 \text{ GeV}$, are found to be 4.14×10^{-9} , 4.15×10^{-9} , 4.12×10^{-9} , 4.13×10^{-9} , 16.57×10^{-9} , $16.65 \times 10^{-9} \text{ GeV}^{-2}$. Comparing with the limits without systematic uncertainties shows that including an overall 5% uncertainty would not weaken the sensitivity remarkably.

5 Summary and conclusions

Lepton flavor violation processes are absent in the SM but appear in many extensions of the SM. In particular, the branching fractions of LFV $\tau^\pm \rightarrow \ell^\pm \ell^\pm \ell'^\mp$, $\ell, \ell' = e, \mu$ decays are increased in various beyond the SM scenarios. In this work, the sensitivity of the future circular electron-positron collider, FCC-ee, to probe the LFV couplings is examined using the $e^-e^+ \rightarrow e^\pm \tau^\mp$ production. To perform the study, an effective Lagrangian approach, in particular, four fermi contact interactions with vector and scalar types are exploited. In order to find the sensitivity, events are generated for four run scenarios of center-of-mass energies of 157.5, 162.5, 240, and 365 GeV with their corresponding benchmarks for the integrated luminosity. The events are generated using `MadGraph5_aMC@NLO` considering ISR effect and passed through `PYTHIA 8` for showering, hadronization, and decay of unstable particles. A fast detector simulation is carried out by `Delphes` using the ILD detector card. The signal final state consists of an isolated electron

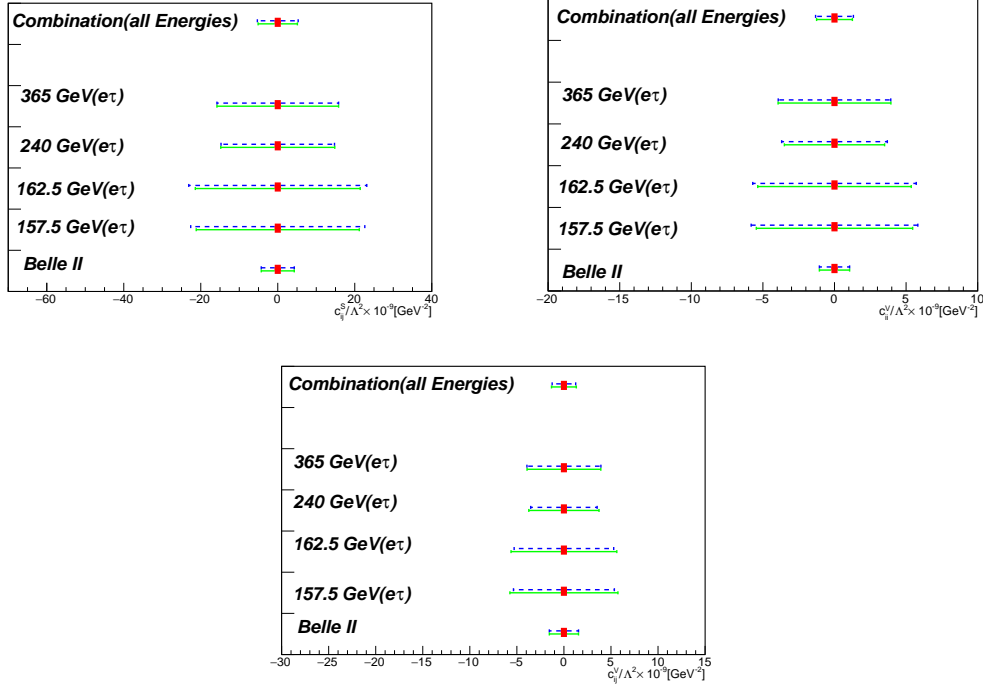


Figure 2: Expected constraints at 95%CL on c_{ij}^S (top left) with c_{LR}^S (dashed-blue) and c_{RL}^S (solid-green), c_{ii}^V (top right) with c_{LL}^V (dashed-blue), c_{RR}^V (solid-green), and c_{ij}^V (bottom) with c_{LR}^V (dashed-blue) and c_{RL}^V (solid-green) from $e^-e^+ \rightarrow e\tau$ for four center-mass-energies are shown. The result of combination of four energies and the prospects from Belle II with 50 ab^{-1} at 90% CL [20] are presented for comparison.

and a τ lepton. In this study, the hadronic decays of the τ lepton are considered for which the branching fraction is around 64%. Based on the final state, the main sources of reducible and irreducible background processes are taken into account. Cuts on the energy of the final electron and the invariant mass of $e\tau$ system are applied to suppress the background contributions. Upper limits at 95% CL on the couplings of various types of LFV couplings have been obtained using the CL_s method for the four center-of-mass energies. Finally, a statistical combination of results obtained at four center-of-mass energies is performed. We show that the statistical combination of four center-of-mass energies increases the sensitivity to the LFV couplings by a factor of two and larger with respect to the limits obtained at $\sqrt{s} = 365 \text{ GeV}$. The results are compared with those obtained from other studies at lepton colliders considering beam polarizations and with prospects from Belle II. The results of combination are competitive with expectations for Belle II with 50 ab^{-1} .

Acknowledgments

S.Tizchang is grateful to Qiang Li for replying the question about implementing ISR in MadGraph5_aMC@NLO. S.M. Etesami is grateful to INSF for the financial support. R. Jafari and S. Tizchang are thankful to the Iran Science Elites Federation for the financial support.

References

- [1] S. L. Glashow, Nucl. Phys. **22**, 579-588 (1961) doi:10.1016/0029-5582(61)90469-2
- [2] S. Weinberg, Phys. Rev. Lett. **19**, 1264-1266 (1967) doi:10.1103/PhysRevLett.19.1264
- [3] S. T. Petcov, Sov. J. Nucl. Phys. **25**, 340 (1977) [erratum: Sov. J. Nucl. Phys. **25**, 698 (1977); erratum: Yad. Fiz. **25**, 1336 (1977)] JINR-E2-10176.
- [4] P. Blackstone, M. Fael and E. Passemar, Eur. Phys. J. C **80**, no.6, 506 (2020) doi:10.1140/epjc/s10052-020-8059-7 [arXiv:1912.09862 [hep-ph]].
- [5] J. R. Ellis, J. Hisano, M. Raidal and Y. Shimizu, Phys. Rev. D **66**, 115013 (2002) doi:10.1103/PhysRevD.66.115013 [arXiv:hep-ph/0206110 [hep-ph]].
- [6] P. Paradisi, JHEP **10**, 006 (2005) doi:10.1088/1126-6708/2005/10/006 [arXiv:hep-ph/0505046 [hep-ph]].
- [7] R. Barbier, C. Berat, M. Besancon, M. Chemtob, A. Deandrea, E. Dudas, P. Fayet, S. Lavignac, G. Moreau and E. Perez, *et al.* Phys. Rept. **420**, 1-202 (2005) doi:10.1016/j.physrep.2005.08.006 [arXiv:hep-ph/0406039 [hep-ph]].
- [8] G. Aad *et al.* [ATLAS], Eur. Phys. J. C **76** (2016) no.5, 232 doi:10.1140/epjc/s10052-016-4041-9 [arXiv:1601.03567 [hep-ex]].
- [9] R. Aaij *et al.* [LHCb], JHEP **02** (2015), 121 doi:10.1007/JHEP02(2015)121 [arXiv:1409.8548 [hep-ex]].
- [10] G. Aad *et al.* [ATLAS], Eur. Phys. J. C **77** (2017) no.2, 70 doi:10.1140/epjc/s10052-017-4624-0 [arXiv:1604.07730 [hep-ex]].
- [11] R. Aaij *et al.* [LHCb], Phys. Lett. B **754** (2016), 167-175 doi:10.1016/j.physletb.2016.01.029 [arXiv:1512.00322 [hep-ex]].
- [12] A. M. Sirunyan *et al.* [CMS], JHEP **01**, 163 (2021) doi:10.1007/JHEP01(2021)163 [arXiv:2007.05658 [hep-ex]].
- [13] G. Aad *et al.* [ATLAS], [arXiv:2010.02566 [hep-ex]].
- [14] A. M. Sirunyan *et al.* [CMS], JHEP **03**, 103 (2020) doi:10.1007/JHEP03(2020)103 [arXiv:1911.10267 [hep-ex]].
- [15] A. M. Baldini *et al.* [MEG], Eur. Phys. J. C **76**, no.8, 434 (2016) doi:10.1140/epjc/s10052-016-4271-x [arXiv:1605.05081 [hep-ex]].
- [16] B. Aubert *et al.* [BaBar], Phys. Rev. Lett. **104**, 021802 (2010) doi:10.1103/PhysRevLett.104.021802 [arXiv:0908.2381 [hep-ex]].
- [17] U. Bellgardt *et al.* [SINDRUM], Nucl. Phys. B **299**, 1-6 (1988) doi:10.1016/0550-3213(88)90462-2
- [18] J. P. Lees *et al.* [BaBar], Phys. Rev. D **81**, 111101 (2010) doi:10.1103/PhysRevD.81.111101 [arXiv:1002.4550 [hep-ex]].

- [19] K. Hayasaka, K. Inami, Y. Miyazaki, K. Arinstein, V. Aulchenko, T. Aushev, A. M. Ba-
kich, A. Bay, K. Belous and V. Bhardwaj, *et al.* Phys. Lett. B **687**, 139-143 (2010)
doi:10.1016/j.physletb.2010.03.037 [arXiv:1001.3221 [hep-ex]].
- [20] E. Kou *et al.* [Belle-II], PTEP **2019**, no.12, 123C01 (2019) [erratum: PTEP **2020**, no.2,
029201 (2020)] doi:10.1093/ptep/ptz106 [arXiv:1808.10567 [hep-ex]].
- [21] H. Aihara *et al.* [ILC], [arXiv:1901.09829 [hep-ex]].
- [22] H. Baer, T. Barklow, K. Fujii, Y. Gao, A. Hoang, S. Kanemura, J. List, H. E. Logan,
A. Nomerotski and M. Perelstein, *et al.* [arXiv:1306.6352 [hep-ph]].
- [23] T. Behnke, J. E. Brau, B. Foster, J. Fuster, M. Harrison, J. M. Paterson, M. Peskin,
M. Stanitzki, N. Walker and H. Yamamoto, [arXiv:1306.6327 [physics.acc-ph]].
- [24] P. N. Burrows *et al.* [CLICdp and CLIC], doi:10.23731/CYRM-2018-002 [arXiv:1812.06018
[physics.acc-ph]].
- [25] P. Roloff *et al.* [CLIC and CLICdp], [arXiv:1812.07986 [hep-ex]].
- [26] M. Aicheler *et al.* [CLIC accelerator], doi:10.23731/CYRM-2018-004 [arXiv:1903.08655
[physics.acc-ph]].
- [27] M. Ahmad, D. Alves, H. An, Q. An, A. Arhrib, N. Arkani-Hamed, I. Ahmed, Y. Bai,
R. B. Feroli and Y. Ban, *et al.* IHEP-CEPC-DR-2015-01.
- [28] IHEP-CEPC-DR-2015-01.
- [29] A. Abada *et al.* [FCC], Eur. Phys. J. ST **228**, no.2, 261-623 (2019) doi:10.1140/epjst/e2019-
900045-4
- [30] J. N. Esteves, J. C. Romao, A. Villanova del Moral, M. Hirsch, J. W. F. Valle and W. Porod,
JHEP **05** (2009), 003 doi:10.1088/1126-6708/2009/05/003 [arXiv:0903.1408 [hep-ph]].
- [31] Y. Cai, T. Han, T. Li and R. Ruiz, Front. in Phys. **6** (2018), 40 doi:10.3389/fphy.2018.00040
[arXiv:1711.02180 [hep-ph]].
- [32] S. Goswami, K. N. Vishnudath and N. Khan, Phys. Rev. D **99** (2019) no.7, 075012
doi:10.1103/PhysRevD.99.075012 [arXiv:1810.11687 [hep-ph]].
- [33] D. Delepine and F. Vissani, Phys. Lett. B **522** (2001), 95-101 doi:10.1016/S0370-
2693(01)01254-0 [arXiv:hep-ph/0106287 [hep-ph]].
- [34] J. I. Illana and T. Riemann, Phys. Rev. D **63** (2001), 053004
doi:10.1103/PhysRevD.63.053004 [arXiv:hep-ph/0010193 [hep-ph]].
- [35] A. Flores-Tlalpa, J. M. Hernandez, G. Tavares-Velasco and J. J. Toscano, Phys. Rev. D **65**
(2002), 073010 doi:10.1103/PhysRevD.65.073010 [arXiv:hep-ph/0112065 [hep-ph]].
- [36] M. A. Perez, G. Tavares-Velasco and J. J. Toscano, Int. J. Mod. Phys. A **19** (2004), 159-178
doi:10.1142/S0217751X04017100 [arXiv:hep-ph/0305227 [hep-ph]].
- [37] P. S. B. Dev, R. N. Mohapatra and Y. Zhang, Phys. Rev. Lett. **120** (2018) no.22, 221804
doi:10.1103/PhysRevLett.120.221804 [arXiv:1711.08430 [hep-ph]].

- [38] P. S. B. Dev, R. N. Mohapatra and Y. Zhang, [arXiv:1902.04773 [hep-ph]].
- [39] A. Goudelis, O. Lebedev and J. h. Park, Phys. Lett. B **707** (2012), 369-374 doi:10.1016/j.physletb.2011.12.059 [arXiv:1111.1715 [hep-ph]].
- [40] A. Vicente, Front. in Phys. **7** (2019), 174 doi:10.3389/fphy.2019.00174 [arXiv:1908.07759 [hep-ph]].
- [41] B. Murakami and T. M. P. Tait, Phys. Rev. D **91** (2015), 015002 doi:10.1103/PhysRevD.91.015002 [arXiv:1410.1485 [hep-ph]].
- [42] G. C. Cho, Y. Fukuda and T. Kono, Phys. Lett. B **789** (2019), 399-404 doi:10.1016/j.physletb.2018.12.056 [arXiv:1803.10475 [hep-ph]].
- [43] J. de Favereau *et al.* [DELPHES 3], JHEP **02** (2014), 057 doi:10.1007/JHEP02(2014)057 [arXiv:1307.6346 [hep-ex]].
- [44] Y. Kuno and Y. Okada, Rev. Mod. Phys. **73** (2001), 151-202 doi:10.1103/RevModPhys.73.151 [arXiv:hep-ph/9909265 [hep-ph]].
- [45] M. Tanabashi *et al.* [Particle Data Group], Phys. Rev. D **98** (2018) no.3, 030001 doi:10.1103/PhysRevD.98.030001
- [46] U. Bellgardt *et al.* [SINDRUM], Nucl. Phys. B **299** (1988), 1-6 doi:10.1016/0550-3213(88)90462-2
- [47] A. M. Baldini *et al.* [MEG], Eur. Phys. J. C **76**, no.8, 434 (2016) doi:10.1140/epjc/s10052-016-4271-x [arXiv:1605.05081 [hep-ex]].
- [48] W. H. Bertl *et al.* [SINDRUM II], Eur. Phys. J. C **47**, 337-346 (2006) doi:10.1140/epjc/s2006-02582-x
- [49] J. Cohen, S. Bar-Shalom and G. Eilam, Phys. Rev. D **94**, no.3, 035030 (2016) doi:10.1103/PhysRevD.94.035030 [arXiv:1602.01698 [hep-ph]].
- [50] H. Khanpour and M. Mohammadi Najafabadi, Phys. Rev. D **95**, no.5, 055026 (2017) doi:10.1103/PhysRevD.95.055026 [arXiv:1702.00951 [hep-ph]].
- [51] Y. Afik, S. Bar-Shalom, J. Cohen and Y. Rozen, Phys. Lett. B **807**, 135541 (2020) doi:10.1016/j.physletb.2020.135541 [arXiv:1912.00425 [hep-ex]].
- [52] Y. Afik, S. Bar-Shalom, A. Soni and J. Wudka, [arXiv:2101.05286 [hep-ph]].
- [53] P. M. Ferreira, R. B. Guedes and R. Santos, Phys. Rev. D **75** (2007), 055015 doi:10.1103/PhysRevD.75.055015 [arXiv:hep-ph/0611222 [hep-ph]].
- [54] M. Greco, T. Han and Z. Liu, Phys. Lett. B **763** (2016), 409-415 doi:10.1016/j.physletb.2016.10.078 [arXiv:1607.03210 [hep-ph]].
- [55] A. Alloul, N. D. Christensen, C. Degrande, C. Duhr and B. Fuks, Comput. Phys. Commun. **185** (2014), 2250-2300 doi:10.1016/j.cpc.2014.04.012 [arXiv:1310.1921 [hep-ph]].
- [56] C. Degrande, C. Duhr, B. Fuks, D. Grellscheid, O. Mattelaer and T. Reiter, Comput. Phys. Commun. **183** (2012), 1201-1214 doi:10.1016/j.cpc.2012.01.022 [arXiv:1108.2040 [hep-ph]].

- [57] J. Alwall, M. Herquet, F. Maltoni, O. Mattelaer and T. Stelzer, JHEP **06**, 128 (2011) doi:10.1007/JHEP06(2011)128 [arXiv:1106.0522 [hep-ph]].
- [58] J. Alwall, C. Duhr, B. Fuks, O. Mattelaer, D. G. Öztürk and C. H. Shen, Comput. Phys. Commun. **197**, 312-323 (2015) doi:10.1016/j.cpc.2015.08.031 [arXiv:1402.1178 [hep-ph]].
- [59] J. Alwall, R. Frederix, S. Frixione, V. Hirschi, F. Maltoni, O. Mattelaer, H. S. Shao, T. Stelzer, P. Torrielli and M. Zaro, JHEP **07**, 079 (2014) doi:10.1007/JHEP07(2014)079 [arXiv:1405.0301 [hep-ph]].
- [60] C. Chen, Z. Cui, G. Li, Q. Li, M. Ruan, L. Wang and Q. s. Yan, [arXiv:1705.04486 [hep-ph]].
- [61] Q. Li and Q. S. Yan, [arXiv:1804.00125 [hep-ph]].
- [62] T. Sjöstrand, S. Ask, J. R. Christiansen, R. Corke, N. Desai, P. Ilten, S. Mrenna, S. Prestel, C. O. Rasmussen and P. Z. Skands, Comput. Phys. Commun. **191** (2015), 159-177 doi:10.1016/j.cpc.2015.01.024 [arXiv:1410.3012 [hep-ph]].
- [63] T. Sjostrand, S. Mrenna and P. Z. Skands, Comput. Phys. Commun. **178** (2008), 852-867 doi:10.1016/j.cpc.2008.01.036 [arXiv:0710.3820 [hep-ph]].
- [64] H. Abramowicz *et al.* [ILD], [arXiv:1912.04601 [physics.ins-det]].
- [65] C. T. Potter, [arXiv:1602.07748 [hep-ph]].
- [66] A. L. Read, J. Phys. G **28**, 2693-2704 (2002) doi:10.1088/0954-3899/28/10/313
- [67] T. Junk, Nucl. Instrum. Meth. A **434**, 435-443 (1999) doi:10.1016/S0168-9002(99)00498-2 [arXiv:hep-ex/9902006 [hep-ex]].
- [68] K. Cranmer *et al.* [ROOT], CERN-OPEN-2012-016.
- [69] G. Aad *et al.* [ATLAS and CMS], JHEP **08**, 045 (2016) doi:10.1007/JHEP08(2016)045 [arXiv:1606.02266 [hep-ex]].
- [70] G. Abbiendi *et al.* [OPAL], Phys. Lett. B **519**, 23-32 (2001) doi:10.1016/S0370-2693(01)01086-3 [arXiv:hep-ex/0109011 [hep-ex]].